Supporting Information

Terbium-modified two-dimensional zirconium-based metal–organic frameworks for photoluminescent detection of nitrite

You-Liang Chen,[a] Cheng-Hui Shen,[a] Chi-Wei Huang,[a] and Chung-Wei Kung *[a]

[a] Department of Chemical Engineering, National Cheng Kung University, Tainan City, Taiwan, 70101.

*Email: cwkung@mail.ncku.edu.tw

To precisely examine the loading of capping benzoate (BA) on the hexa-zirconium nodes of the as-synthesized BA-ZrBTB and ZrBTB, the MOF sample was digested in the mixture of concentrated D_2SO_4 and d_6-DMSO. The obtained ^1H NMR spectra are shown in Figure S1. The three sets of characteristic doublet and triplet peaks located at around 7.3, 7.4, and 7.7 ppm observed in Figure S1(a) correspond to the five protons from the capping benzoate.[1] In addition, the peaks at around 7.85 ppm originate from fifteen protons in the H_3BTB linker.[2, 3] By integration, the ratio between the benzoate and BTB in BA-ZrBTB was calculated as 1.6:1, which indicates that there are 3.2 capping benzoate on each hexa-zirconium node in BA-ZrBTB; this ratio is similar to that of BA-ZrBTB synthesized by the same synthetic protocol reported previously.[4] After the protonation, as shown in Figure S1(b), no signals from BA can be observed in the NMR spectrum of ZrBTB, confirming the successful removal of all capping benzoate from the nodes during the HCl/DMSO treatment.

Tb-ZrBTB-40, Tb-ZrBTB-80, and Tb-ZrBTB-120 were also digested in the mixtures of concentrated D_2SO_4 and d_6-DMSO to acquire their full ^1H NMR spectra. As shown in Figure S2(a-c), the peaks at around 13 ppm and 2.5 ppm are the characteristic signals of carboxyl groups and DMSO, respectively. In addition, characteristic peaks of H_3BTB and acetate can be observed in

all of these spectra (also see Figure S2(d-f)). The presence of coordinated acetate originates from the use of terbium acetate as the precursor during the installation of terbium. It should be noticed that a trace amount of residual formate, presumably generated from the decomposition of DMF during the synthesis, can be observed in the spectra at around 8 ppm.[1]

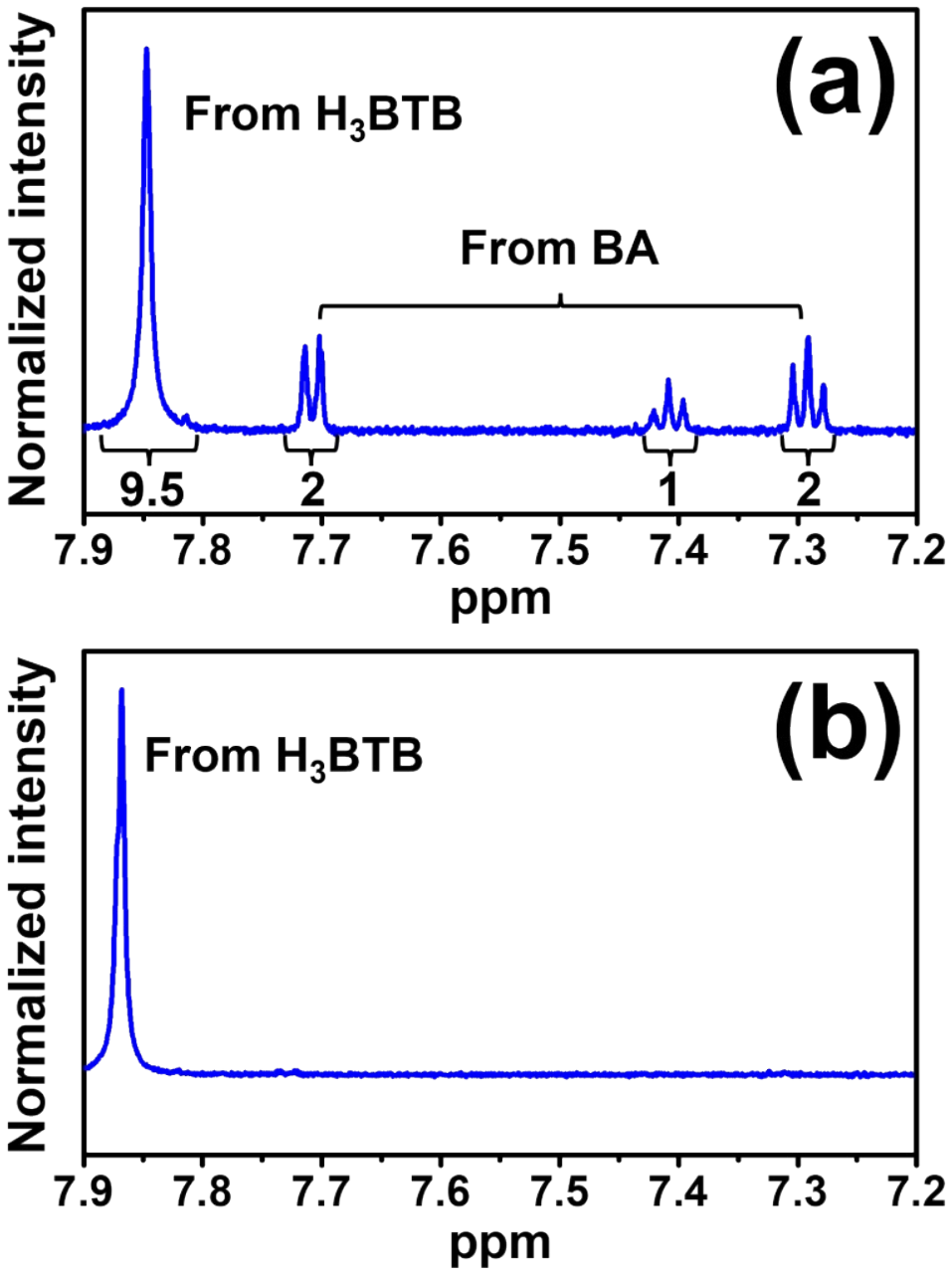

Figure S1. ^{1}H NMR spectra of (a) BA-ZrBTB, and (b) ZrBTB.

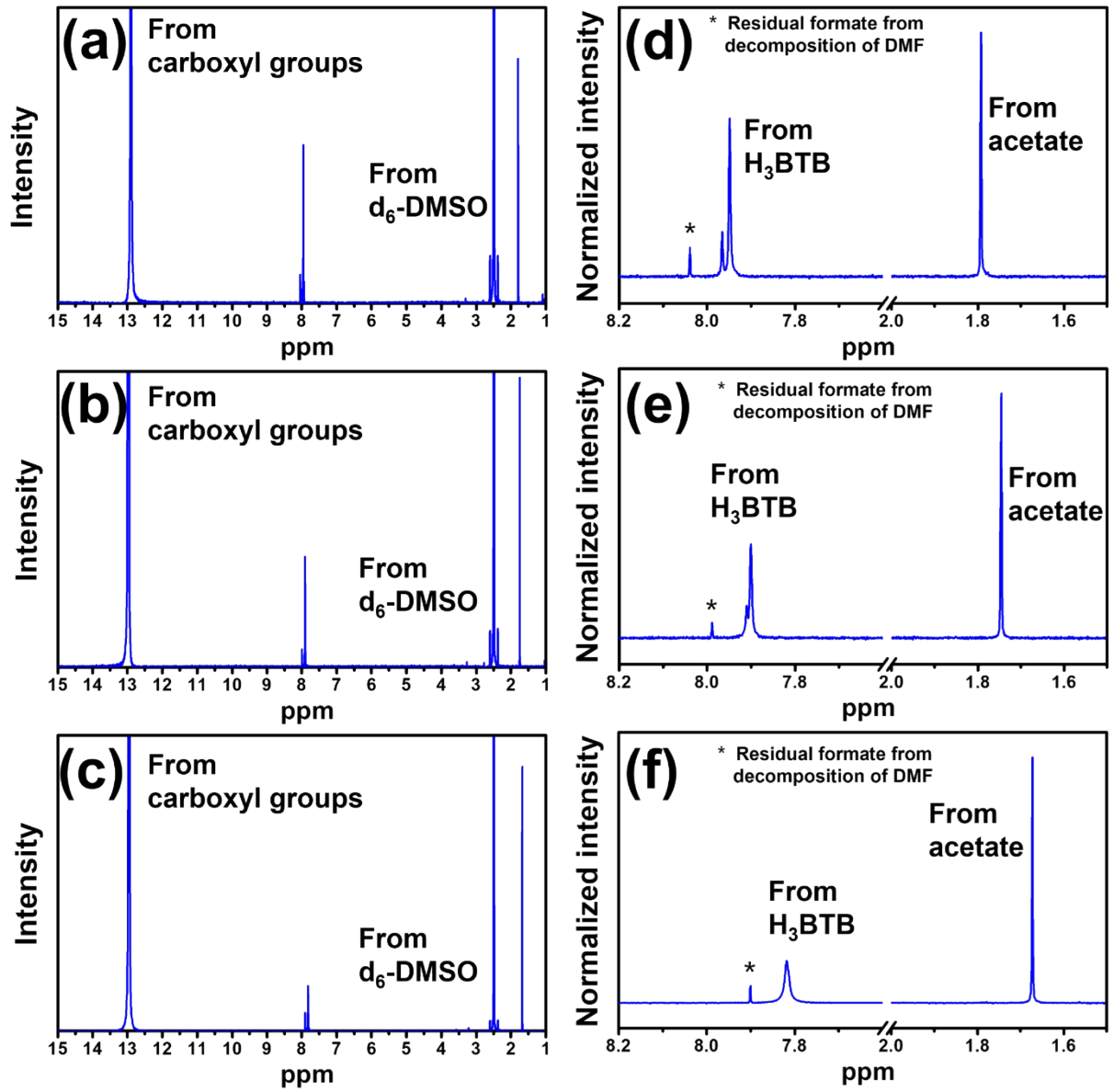

Figure S2. Full ^{1}H NMR spectra of (a) Tb-ZrBTB-40, (b) Tb-ZrBTB-80, and (c) Tb-ZrBTB-120. ^{1}H NMR spectra enlarged from (a), (b), and (c) are shown in (d), (e), and (f), respectively.

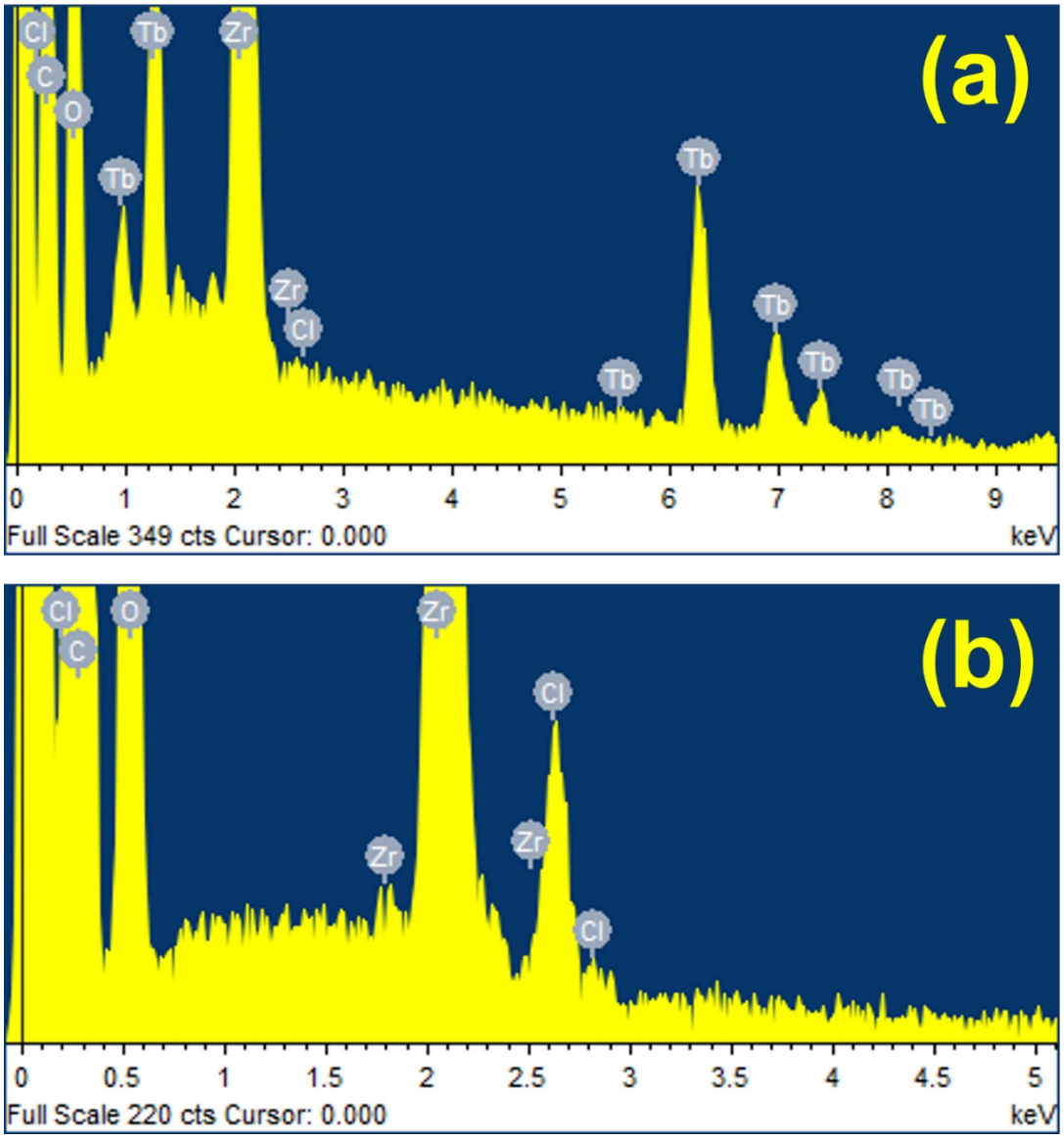

Figure S3. EDS spectra of (a) Tb-ZrBTB-120, and (b) ZrBTB.

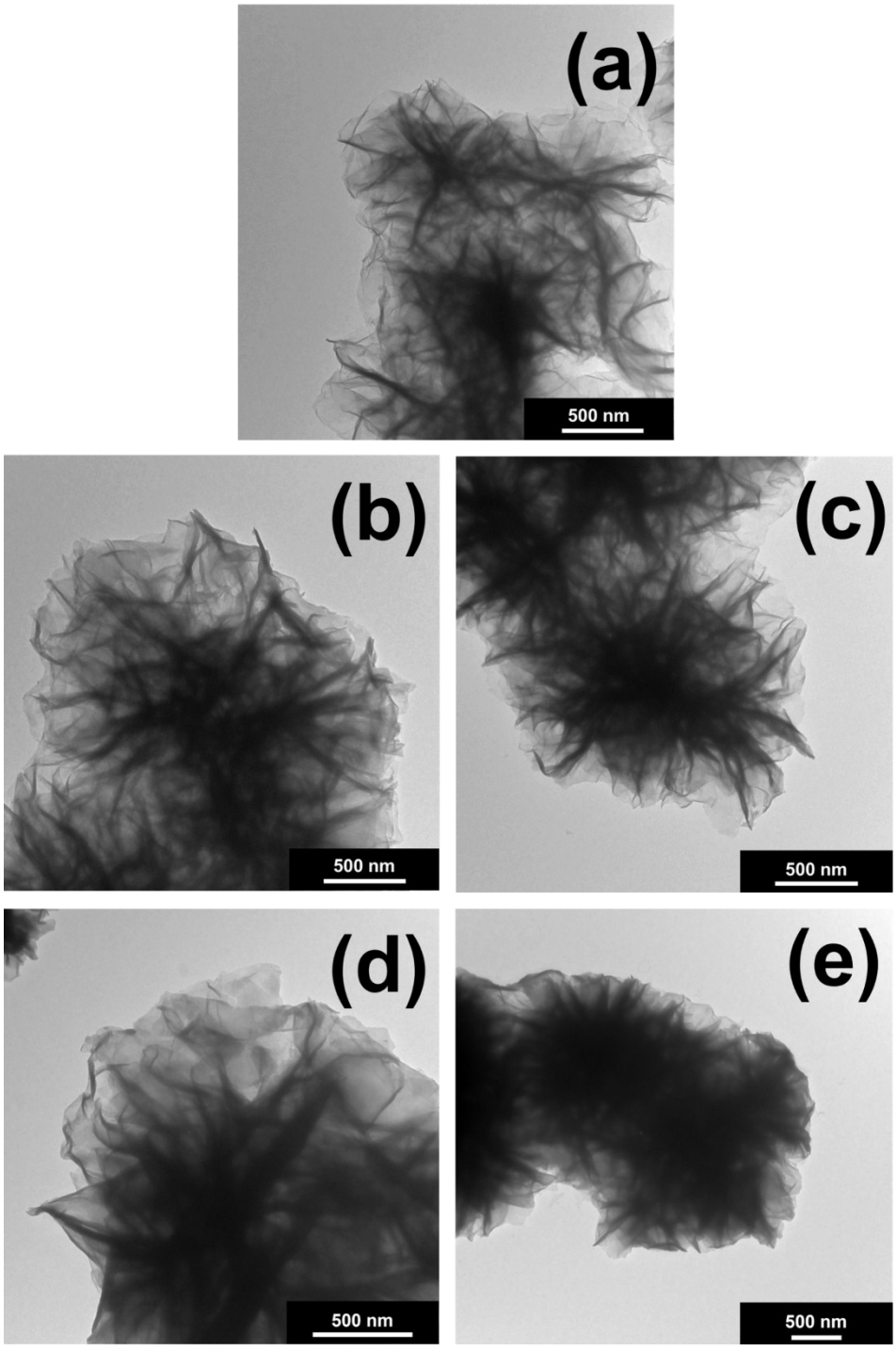

Figure S4. Representative TEM images of (a) BA-ZrBTB, (b) ZrBTB, (c) Tb-ZrBTB-40, (d) Tb-ZrBTB-80, and (e) Tb-ZrBTB-120.

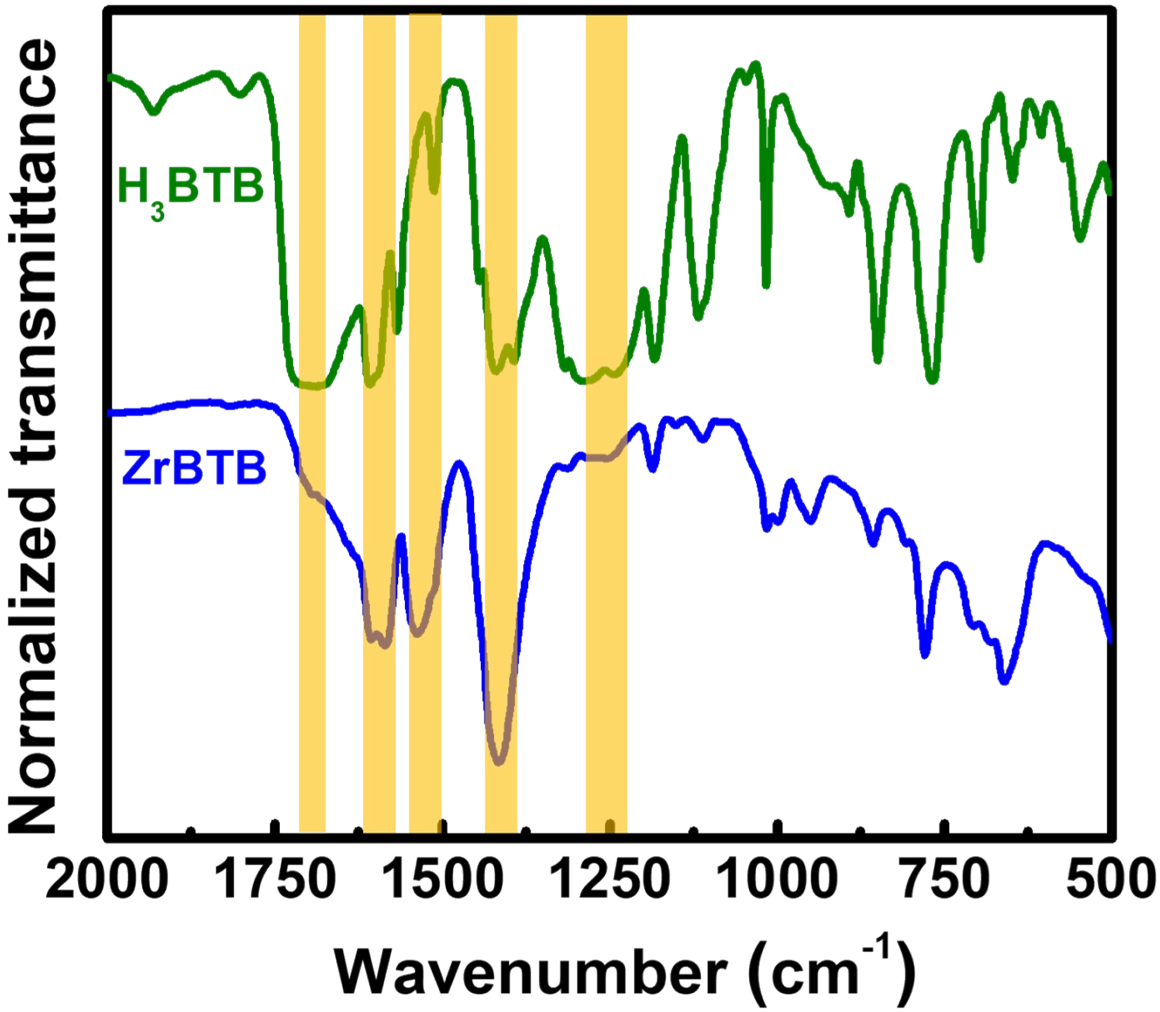

Figure S5. FTIR spectra of H_3BTB and ZrBTB. The characteristic peaks of H_3BTB are highlighted in orange.

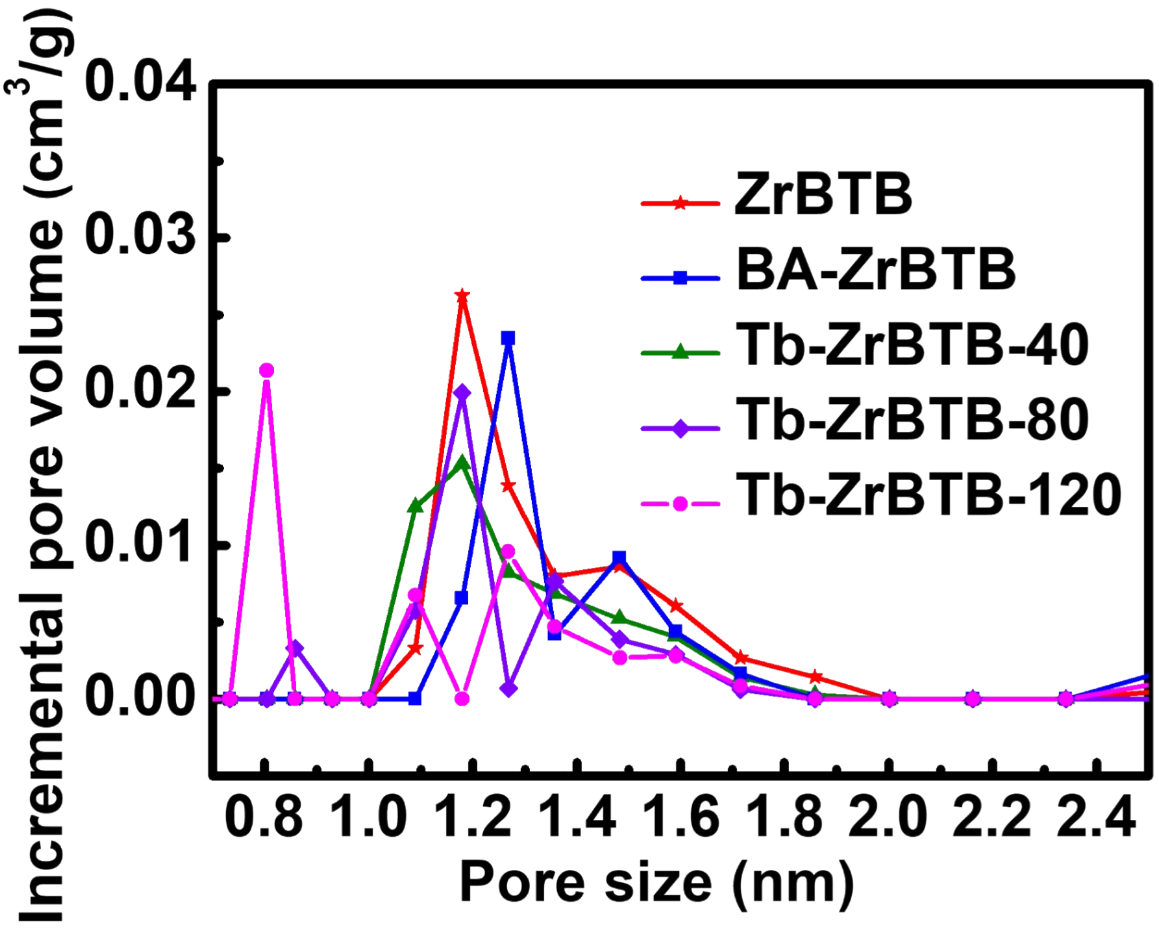

Figure S6. DFT pore size distributions of ZrBTB, BA-ZrBTB, Tb-ZrBTB-40, Tb-ZrBTB-80, and Tb-ZrBTB-120 were calculated from the isotherms shown in Figure 4 of the main text by using linear DFT model with slit pore.

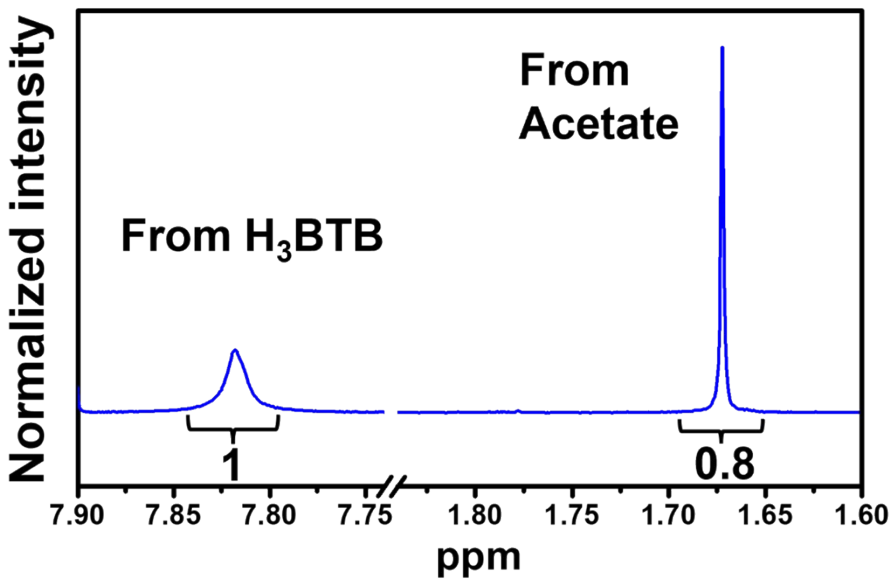

Figure S7. ^{1}H NMR spectrum of Tb-ZrBTB-120. Peaks located at 7.82 ppm and 1.67 ppm correspond to fifteen protons in BTB and three protons in acetate, respectively. Calculated molar ratio between acetate and BTB = 4:1.

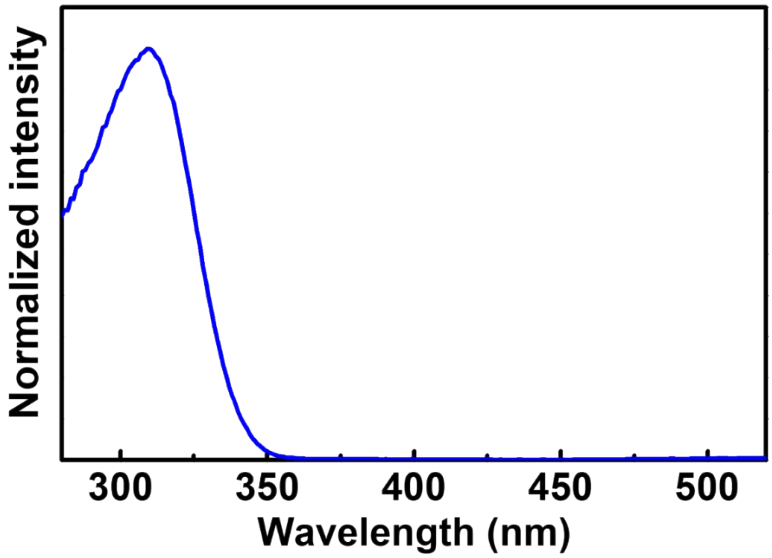

Figure S8. Excitation spectrum of Tb-ZrBTB-120 at an emission wavelength of 543 nm. The solution is composed of water and ethanol (v:v = 1:1). Concentration of the MOF-based solid is 0.2 mg/mL.

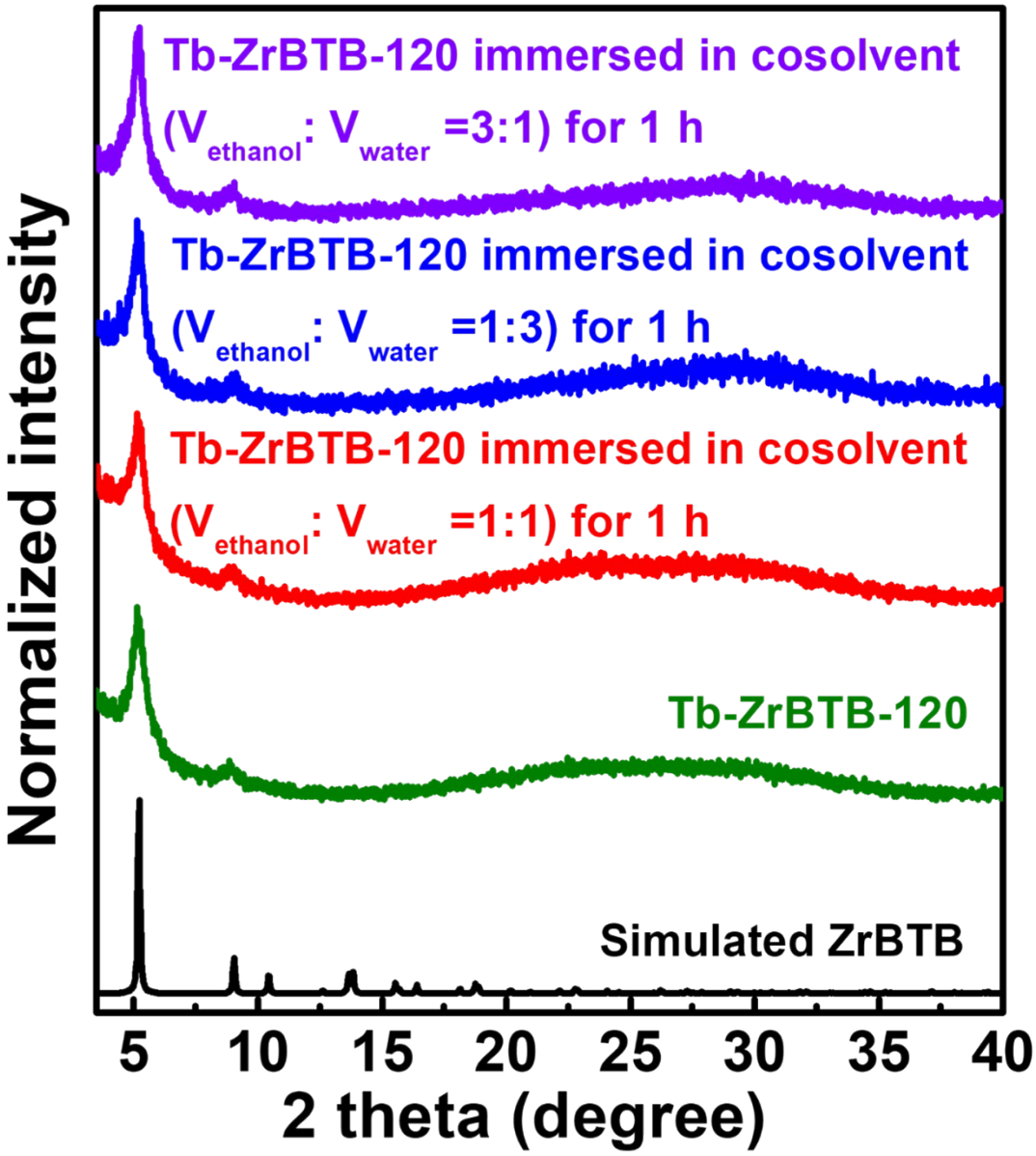

Figure S9. PXRD patterns of Tb-ZrBTB-120 which was immersed in the cosolvent (ethanol and water, v:v = 3:1, 1:1, or 1:3) for 1 h followed by the successive washing with water and acetone for three times sequentially. Pattern of the fresh Tb-ZrBTB-120 and the simulated pattern of ZrBTB are also shown.

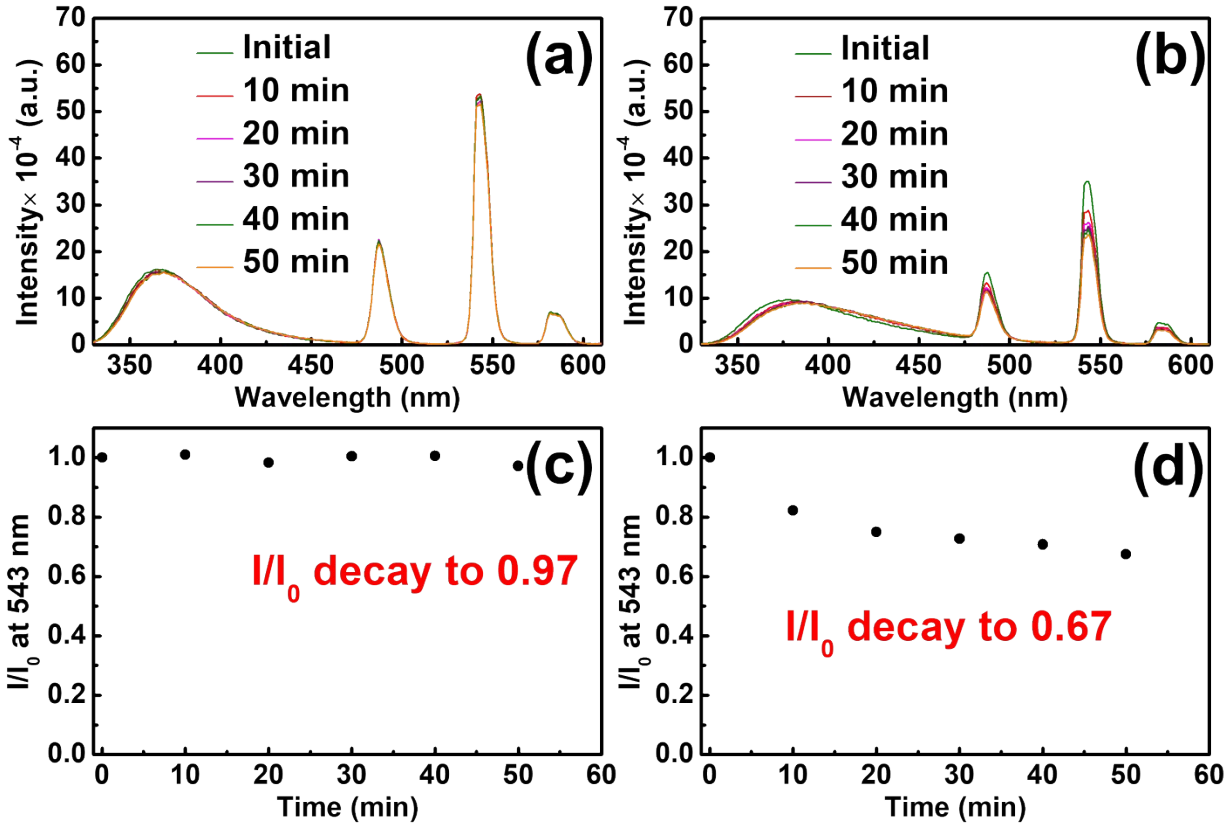

Figure S10. Emission spectra of Tb-ZrBTB-120 measured in (a) cosolvent (water and ethanol, v:v = 1:1) and (b) pure water, collected at different time. The photoluminescent decay in (c) cosolvent and (d) pure water, extracted from (a) and (b) at the wavelength of 543 nm. I and I_0 stand for intensity and initial intensity, respectively. Concentration of Tb-ZrBTB-120 is 0.2 mg/mL.

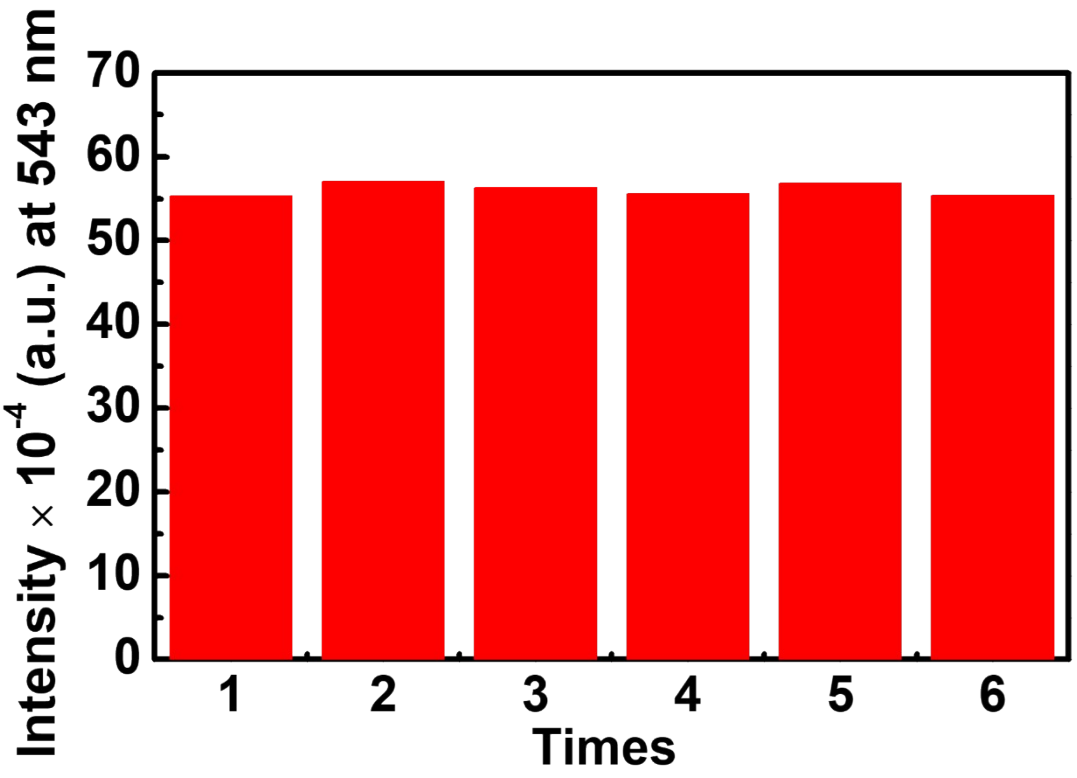

Figure S11. Result of six parallel photoluminescent tests of Tb-ZrBTB-120 suspended in the cosolvent (water and ethanol, v:v = 1:1) without adding nitrite. Concentration of Tb-ZrBTB-120 is 0.2 mg/mL.

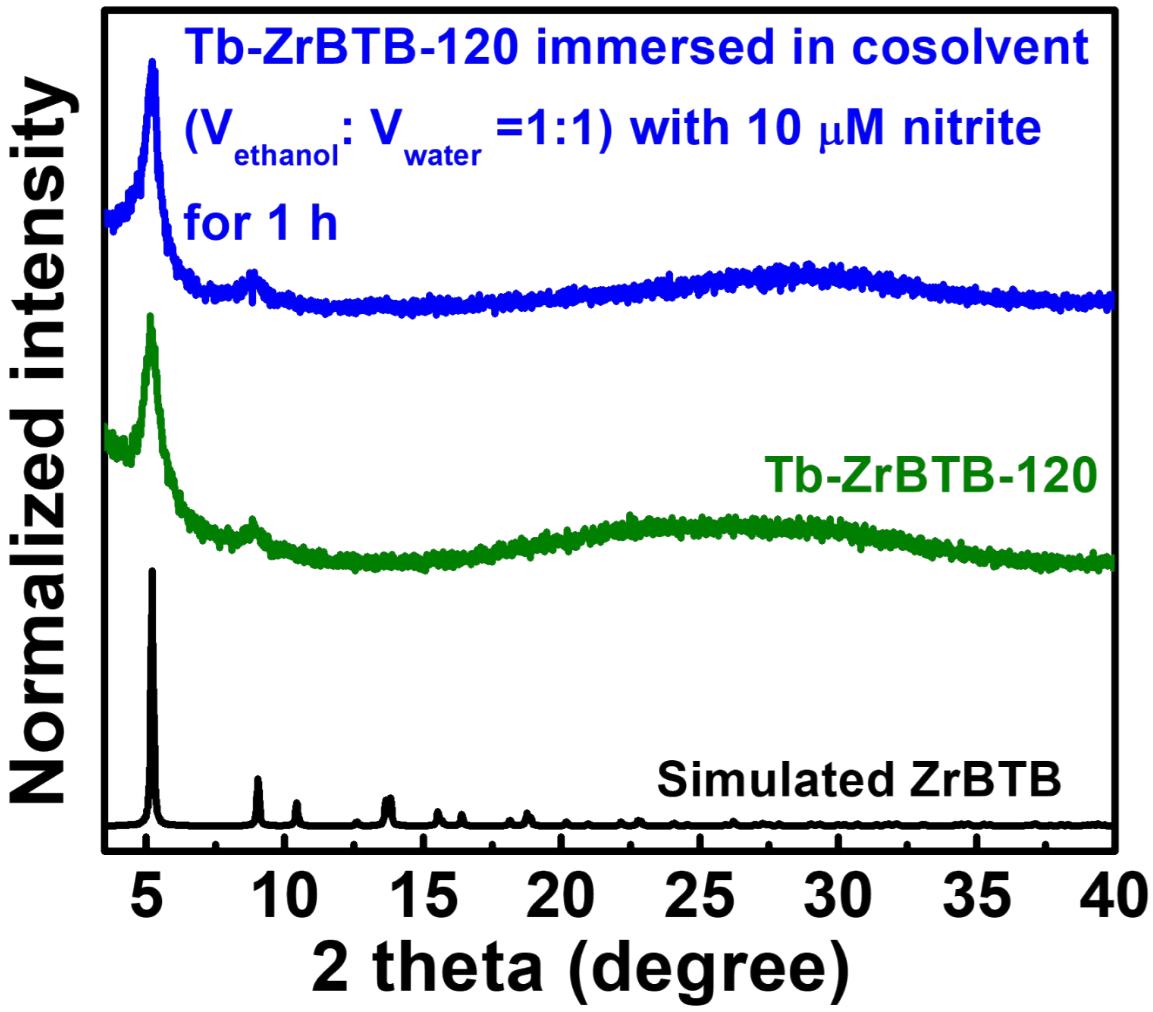

Figure S12. PXRD pattern of Tb-ZrBTB-120 which was immersed in the nitrite containing cosolvent (water and ethanol, v:v = 1:1, with 10 μM of nitrite) for 1 h followed by the successive washing steps with cosolvent and acetone for three times respectively before drying. Pattern of the fresh Tb-ZrBTB-120 and the simulated pattern are also shown.

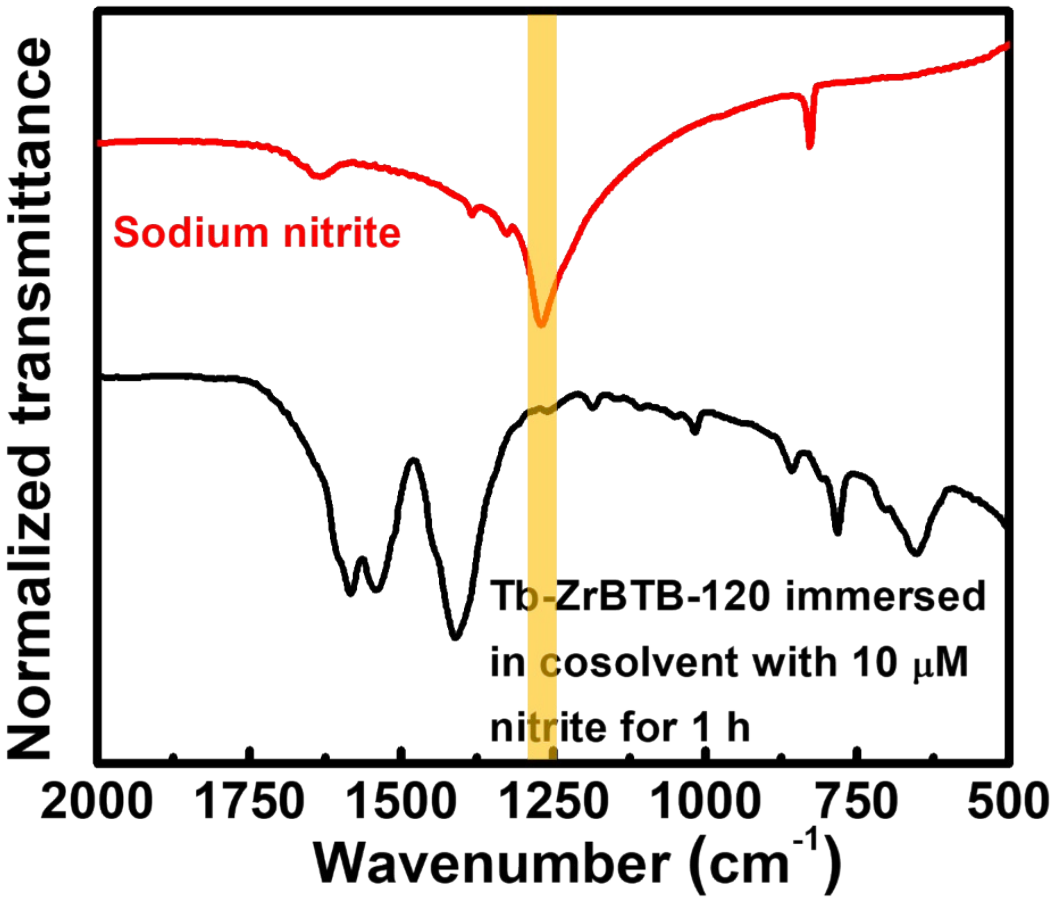

Figure S13. FTIR spectra of sodium nitrite and Tb-ZrBTB-120 which was immersed in the nitrite containing cosolvent (water and ethanol, v:v = 1:1, with 10 μM of nitrite) for 1 h followed by the successive washing steps with cosolvent and acetone for three times respectively before drying. The characteristic peak of sodium nitrite is highlighted in orange.

Table S1. Partial list of the reported photoluminescent nitrite sensors and the comparison between their sensing performances and that of the Tb-ZrBTB-120-based nitrite sensor in this work.

Active material	Performance		Reference
	LOD (μM)	K_{sv} (M^{-1})	
UiO-66-NH_2	77	-	[5]
Eu^{3+}@UiO-66-$(COOH)_2$	0.69	-	[6]
N-CDs [a]	0.65	-	[7]
UiO-66-NH_2-Cit [b]	-	26000	[8]
CQD-Tb^{3+} [c]	0.002	670000	[9]
Tb^{3+}@In-MOF	-	53000	[10]
Tb-MOF	0.028	482000	[11]
U–Tb–OBBA [d]	0.3	-	[12]
TA/11-MU–Au NDs [e]	0.04	480000	[13]
Tb-ZrBTB-120	0.08	472000	This work

[a] N-CDs = Nitrogen-doped carbon dots

[b] Cit = Citric acid

[c] CQD = Carbon quantum dots

[d] U = 5-fluorouracil, OBBA = 4,4'-oxybis(benzoic acid)

[e] TA = Tetradecanoic acid, 11-MU = 11-mercaptoundecanol, NDs = Nanodots

References:

1. C.-H. Shen, Y.-H. Chen, Y.-C. Wang, T.-E. Chang, Y.-L. Chen and C.-W. Kung, *Phys. Chem. Chem. Phys.*, 2022, **24**, 9855-9865.
2. M. Padmanaban, P. Müller, C. Lieder, K. Gedrich, R. Grünker, V. Bon, I. Senkovska, S. Baumgärtner, S. Opelt and S. Paasch, *Chem. Commun.*, 2011, **47**, 12089-12091.
3. Y.-B. Zhang, H. Furukawa, N. Ko, W. Nie, H. J. Park, S. Okajima, K. E. Cordova, H. Deng, J. Kim and O. M. Yaghi, *J. Am. Chem. Soc.*, 2015, **137**, 2641-2650.
4. Y. Wang, L. Feng, J. Pang, J. Li, N. Huang, G. S. Day, L. Cheng, H. F. Drake, Y. Wang, C. Lollar, J. Qin, Z. Gu, T. Lu, S. Yuan and H. C. Zhou, *Adv. Sci.*, 2019, **6**, 1802059.
5. X. Hao, Y. Liang, H. Zhen, X. Sun, X. Liu, M. Li, A. Shen and Y. Yang, *J. Solid State Chem.*, 2020, **287**, 121323.
6. Y. Li, Y. Zhao, W. Zhang, K. Shao and H. Zhou, *Z. Anorg. Allg. Chem.*, 2021, **647**, 1091-1095.
7. J. Jing, L. Wen-Jing, L. Lin, J. Yuan, G. Yi-Fang and S. Shao-Min, *Chinese J. Anal. Chem.*, 2019, **47**, 560-566.
8. S. Zhu, L. Zhao and B. Yan, *Microchem. J.*, 2020, **155**, 104768.
9. H. Wu and C. Tong, *Anal. Chem.*, 2020, **92**, 8859-8866.
10. J.-X. Wu and B. Yan, *Ind. Eng. Chem. Res.*, 2018, **57**, 7105-7111.
11. H. Min, Z. Han, M. Wang, Y. Li, T. Zhou, W. Shi and P. Cheng, *Inorg. Chem. Front.*, 2020, **7**, 3379-3385.
12. Z. Qi, Q. You and Y. Chen, *Anal. Chim. Acta*, 2016, **902**, 168-173.
13. W.-Y. Chen, C.-C. Huang, L.-Y. Chen and H.-T. Chang, *Nanoscale*, 2014, **6**, 11078-11083.